EUROFUSION WPJET1-PR(14) 12684

C Guillemaut et al.

Ion target impact energy during Type I ELMs in JET ITER-like Wall

Preprint of Paper to be submitted for publication in
Plasma Physics and Controlled Fusion

This work has been carried out within the framework of the EUROfusion Consortium and has received funding from the Euratom research and training programme 2014-2018 under grant agreement No 633053. The views and opinions expressed herein do not necessarily reflect those of the European Commission.

Ion target impact energy during Type I ELMs in JET ITER-like Wall

C. Guillemaut[1], A. Jardin[1], J. Horacek[2], A. Autricque[1],
G. Arnoux[3], J. Boom[4], S. Brezinsek[5], J. Coenen[5], E. De La Luna[6], S. Devaux[7], T. Eich[4], D.Harting[3],
*B. Lipschultz[8], G.F. Matthews[3], D. Moulton[9], M. Stamp[3] and JET contributors**

EUROfusion Consortium, JET, Culham Science Centre, Abingdon, OX14 3DB, UK
[1]CEA, IRFM, F-13108 Saint-Paul-lez-Durance, France
[2]IPP.CR, Institute of Plasma Physics AS CR, Za Slovankou 3, 182 21 Praha 8, Czech Republic
[3]CCFE, Culham Science Centre, Abingdon OX14 3DB, UK
[4]Max-Planck-Institut fur Plasmaphysik, Boltzmannstr. 2, D-85748 Garching, Germany
[5]Instiut für Energie und Klimaforschung - Plasmaphysik, Forschungszentrum Jülich, 52425 Jülich, Germany
[6]Laboratorio Nacional de Fusión,CIEMAT, 28040 Madrid, Spain
[7]Institut Jean Lamour, UMR7198 CNRS - Université de Lorraine, F-54506 Vandoeuvre-les-Nancy Cedex, France.
[8]YPI, University of York, York YO10 5DQ, UK
[9]Aalto University, Tekes, Otakaari 4, 02015 Espoo, Finland

Abstract

The ITER baseline scenario, with 500 MW of DT fusion power and Q = 10, will rely on a Type I ELMy H-mode, with ΔW = 0.7 MJ mitigated ELMs. Tungsten (W) is the material now decided for the divertor plasma-facing components from the start of plasma operations. W atoms sputtered from divertor targets during ELMs are expected to be the dominant source under the partially detached divertor conditions required for safe ITER operation. W impurity concentration in the plasma core can dramatically degrade its performance and lead to potentially damaging disruptions. Understanding the physics of plasma-wall interaction during ELMs is important and a primary input for this is the energy of incoming ions during an ELM event. In this paper, coupled Infrared thermography and Langmuir Probe (LP) measurements in JET-ITER-Like-Wall (ILW) unseeded H-mode experiments with ITER relevant ELM energy drop have been used to estimate the impact energy of deuterium ions (D^+) on the divertor target. This analysis gives an ion energy of several keV during ELMs, which makes D^+ responsible for most of the W sputtering in unseeded H-mode discharges. These LP measurements were possible because of the low electron temperature (T_e) during ELMs which allowed saturation of the ion current. Although at first sight surprising, the observation of low T_e at the divertor target during ELMs is consistent with the "Free-Streaming" kinetic model which predicts a near-complete transfer of parallel energy from electrons to ions in order to maintain quasi-neutrality of the ELM filaments while they are transported to the divertor targets.

** See the Appendix of F. Romanelli et al., Proceedings of the 25th IAEA Fusion Energy Conference 2014, Saint Petersburg, Russia*

1. Introduction

The ITER baseline scenario, with 500 MW of DT fusion power and Q = 10, will rely on a Type I ELMy H-mode, with ΔW = 0.7 MJ mitigated ELMs, see [1]. Partial divertor detachment with nitrogen (N), neon (Ne) or argon (Ar) impurity seeding will also be required to maintain the inter-ELM power load at managable level. Tungsten (W) is the material now decided for the divertor plasma-facing components from the start of plasma operations. W atoms sputtered from divertor targets during ELMs are expected to be the dominant source under the partially detached divertor conditions envisaged for ITER as the steady-state source is switched off between ELMs due to energetic threshold of the physical sputtering processes involving deuterium (D), beryllium (Be) and impurity ions. W impurity concentration in the plasma core above 10^{-5} can degrade fusion performance and may lead to potentially damaging disruptions, see [2]. Understanding the physics of plasma-wall interaction during ELMs is important and a primary input for this is the energy of incoming ions during an ELM event.

The JET-ITER-Like-Wall (ILW) [3] comprises a W divertor and beryllium (Be) main chamber wall thus matching the material configuration planned for ITER. Due to the high energy threshold for physical sputtering of W by D ions (D^+), the dominant Be ion species, Be^{2+}, contributes to W sputtering in the divertor between ELMs (inter-ELM), see [4]. During ELM events, sputtering by D^+ could significantly contribute to W sputtering if the impact energy is sufficiently high and the concentration of Be is as low as observed in the JET-ILW. According to TRIM calculations for perpendicular impact [5] shown on Fig. 1, if Be^{2+} and D^+ both have a target impact energy (E_i) of ~ 1 keV, they rise their respective W sputtering yield up to $Y_{Be/W}$ ~ 0.1 and $Y_{D/W}$ ~ 0.01. According to [4], in most JET-ILW experiments, the Be concentration in the impinging target ion flux is typically ~ 1 % which means that D^+ could potentially produce ~ 10 times more W sputtering than Be^{2+} during an ELM with ΔW = 0.7 MJ. Therefore, determining E_i experimentally during ELMs is important for verifying whether W sputtered by D^+ is dominant or not. If it is, then the task of modelling the W source term during ELMs becomes simpler given that it is difficult to precisely measure the Be content and charge state mix in the scrape-off layer (SOL) during an ELM or to predict it reliably.

A series of high power unseeded H-Mode discharges performed in JET-ILW (see Table 1) during the W melting experiments [6] has been studied for this purpose. They have been chosen for the range of pedestal electron temperatures (T_e^{ped}) they explore and for the ITER relevance of the energy of their Type I ELMs (up to 0.3 MJ). The divertor configuration used in these experiments features a vertical inner target with a horizontal outer target (OT), see Fig. 2. The present work has been focused on the use of high time resolution Infrared thermography (IR), Langmuir Probes (LP) and Electron Cyclotron Emission (ECE) measurements to study the conditions on the horizontal OT during ELMs and compared to the pedestal conditions.

Before discussing the experimental results, it was essential to confirm that ion saturation current densities (J_{sat}) measured by LP remain valid during ELMs by comparing to D_α spectroscopy measurements (Section 2) and by analyzing current-voltage (I-V) characteristic reconstruction from LP during ELMs (Section 3). The positive outcome of this analysis meant that it was possible to estimate E_i by coupling IR and LP measurements and compare it to pedestal conditions measured by ECE (Section 4). To conclude, we discuss the consequences of these estimates on W sputtering due to D^+ and Be^{2+} (Section 5) and also the extent to which our results are consistent with the theory of ELM events as represented in kinetic models.

2. Ion flux measurements with LP and D_α spectroscopy during ELMs

It could be argued that the current measured by single LP cannot be used during ELMs to obtain a proper J_{sat} value, since the electrons may simply have too much parallel energy to be repelled by the biased surface of the probes [7]. For example, the LP at JET cannot be biased to more than -170 V, which would be insufficient to repel electrons with a parallel energy of the order of 0.5 - 1 keV which are typical of the T_e^{ped} in JET-ILW. In this hypothetical case, the current measured by the probes would not saturate and the maximum ion flux obtained at -170 V would still be significantly lower than the real flux.

LP are routinely used in high power H-Mode JET-ILW experiments like the ones listed in Table 1. In these cases, the LP voltage was swept between +30 V and -140 V every 2.4 ms with an acquisition rate of 100 kHz for the current and voltage measurements. Thus, if the electrons had a sufficiently low energy to be repelled by biased LP in the divertor, the saturated ion branch of the I-V characteristic would provide a J_{sat} measurement with 10 μs time resolution. This should allow precise description of Type I ELMs since they typically last for a period of ~ 1 ms.

As a first verification of the accuracy of the LP ion current measurements during ELMs, a comparison has been made between the measurements from D_α spectroscopy and the set of LP on the OT (Tile 5 in Fig. 2). It has been assumed that the intensity of D_α line emission from local D recycling is proportional to the ion flux falling on the area of the outer strike point seen by the filterscope equiped with narrowband D_α filters. The filterscope used to measure the D_α is absolutely calibrated and the recycling coefficient is assumed to be R = 1. It has been found that the ratio between the total number of Balmer photons per second in the field of view and the ion flux integrated over the equivalent volume of plasma is ~ 20 for the series of discharges of Table 1. This is consistent with expected values from ADAS and previous studies on JET [8,9] for inverse photon efficiency which is relatively independent of electron temperature (T_e) in the domain explored.

The ELMs are extremely reproducible in these experiments and so an ELM detection algorithm coupled with a coherent averaging method [10] has been applied to the integrated signals from LP and D_α spectroscopy to obtain a typical ELM ion flux signature for a given discharge. The example given in Fig. 3 for the particular discharge #84782 is representative of the other cases listed in Table 1. It appears that the discrepancy between both measurements of ion flux is not higher than ~ 50 % during the averaged ELM phase which suggests that LP measurements seem to be accurate in these conditions. Whilst reasonable, this level of discrepancy can be explained by the secondary electron emissions affecting the LP measurements and/or the slight density dependence of the photon efficiency per incoming ion, see [8,9].

One interesting feature of the ELMs in this series of discharges is that they are always followed by a short and intense particle pulse which is not associated with a significant power deposition, see Fig. 4. As shown by Be II and W I spectroscopy, this low energetic peak which occurs ~ 8 ms after the ELM event is not responsible for any significant sputtering on the targets. This phenomenon which may be related to thermal desorption of gas stored in the surface [4,11] is very common in JET-ILW and has also been observed on ASDEX-Upgrade.

Similar particle fluxes measured by LP and D_α spectroscopy (assuming R = 1) during ELMs is an indication that the parallel energy of the electrons at the targets may be sufficiently low to allow their repulsion by the biased LP surfaces and therefore the saturation of the measured current when the applied voltage is high enough. If there was no current saturation during ELMs, the ion flux measured by the LP should be much lower than the D_α spectroscopy measurement on Fig. 3. It is therefore a positive result to see that the opposite situation occurs in reality. Better evidence would be the direct observation of LP current saturation during ELMs which is the subject of the next section.

3. Direct observation of LP current saturation during ELMs

As an example, peak ELM current values (I in A) with their associated voltages (V in V) have been accumulated over the entire discharge #84782 for the LP closest to the strike point (see Probe 13 on Fig. 1) to reconstruct the typical I-V characteristic associated with these conditions. The standard exponential 3-parameter fit, equation (1), has been applied to the coherently averaged raw data where T_e is in eV, the floating potential V_f is in V and the ion saturation current I_{sat} is in A:

$$I = I_{sat}(1 - \mathrm{e}^{\frac{V - V_f}{T_e}}). \quad (1)$$

As shown on Fig. 5, it appears that in these conditions, the I-V characteristic reconstruction from Probe 13 does saturate. The associated target T_e is of the order of 20 – 30 eV, which is sufficiently low to allow the repulsion of the electrons and an accurate measurement of the target ion flux during ELMs, as already suggested by the comparison with D_α measurements. It is worth mentioning that target T_e of the same order of magnitude have already been observed on TCV during ELMs [10] using the same method. As shown in Fig. 6, before the ELM, T_e^{ped} measured by ECE is of the order of ~ 1 keV which makes the observation at first sight rather surprising given that during an ELM one can think that the divertor target becomes connected along a magnetic flux tube to a plasma with the same T_e as the pedestal. However, low target T_e during ELMs – of the order of the inter-ELM value – are actually consistent with the "Free-Streaming" model for the description of parallel ELM transport, see [12-14]. The quasi-neutrality of ELM filament parallel transport forces the electrons to transfer most of their parallel energy to the ions on their way to the targets to avoid the appearance of strong electric fields between two decoupled populations of ions and electrons. Therefore, the quasi-neutral ELM filaments are expected to strike the targets with high parallel energy ions and low parallel energy electrons.

Thus, the coupling of accurate high time resolution particle flux measurements from the LP and heat flux measurements from IR cameras should in principle give access to reasonable estimates of E_i during Type I ELMs.

4. E_i estimates during ELMs and relation with pedestal conditions

Fast LP and IR camera measurements have a time resolution of respectively 10 µs for J_{sat} and 200 µs for $q_\perp$ which should be sufficient to resolve the Type I ELMs (~ 1 ms duration) for the series of discharges listed in Table 1. Since both measurements appear to be reliable during ELMs (see [15] for the use of IR in these conditions), they can be coupled to estimate E_i as follows:

$$E_i \approx \frac{q_\perp}{J_{sat} \sin\theta_\perp} \tag{2}$$

assuming that $q_{\perp,i}$ and $q_{\perp,e}$, the respective perpendicular ion and electron heat flux densities in $MW.m^{-2}$, are such as:

$$q_\perp = q_{\perp,i} + q_{\perp,e} \approx q_{\perp,i} \tag{3}$$

with $\theta_\perp$ the field line angle on the OT (~ 2 - 3º here). Since in the JET-ILW, the fast IR camera looks mainly at the OT which also appears to have the best LP coverage, the present study has been focused on this particular area of the divertor.

As already described, the respective J_{sat} and $q_{\perp}$ measurements from LP and IR at the strike point position (Probe 13 in Fig. 2) have been coherently averaged over the discharge #84782 to obtain the typical ELMy E_i signature shown in Fig. 7. Around ~ 200 ELMs have been cumulated and this averaging starts 2 ms before the ELM event and end 5 ms after. In this example, it can be seen that the peak E_i during the ELM ($E_{i,max}$) and the T_e^{ped} before the ELM crash ($T_{e,\max}^{ped}$) are such as:

$$E_{i,\max} \approx \alpha T_{e.\max}^{ped} \tag{4}$$

with $T_{e,\max}^{ped} \approx$ 1 keV and $\alpha \approx$ 5 here.

Both values have been compared for the other discharges of Table 1 using the same ELM detection algorithm and coherent averaging method and the result is shown on Fig. 8. It appears clearly that the simple linear dependence shown in equation (4) describes quite well the experimental behavior. In [14], if equation (36) is inserted in equation (34) and if the ion pedestal temperature (T_i^{ped}) is such as $T_i^{ped} \approx T_e^{ped}$, the "Free-Streaming" model [12-14] predicts a factor α = 4.23 between $E_{i,max}$ and $T_{e,\max}^{ped}$, which is reasonably close to the experimental value. This confirms that $T_{e,\max}^{ped}$ is the only information required to have access to $E_{i,max}$ during ELMs. Therefore, based on our measurements, it can be concluded that a value of α in the range 4 – 5, provides a good estimate of $E_{i,max}$.

5. Dominant contribution from D^+ to W sputtering

Now that E_i can be experimentally determined for the main plasma species, the relative importance of the different sputtering processes occurring in the unseeded H-mode discharges studied here (see Table 1) can be calculated. Some simplifications will be made to facilitate the analysis and focus the discussion on the orders of magnitude of the W sputtering due to D^+ and Be^{2+} in ELM and inter-ELM conditions.

It can be deduced from Fig. 8 that $E_{i,max}$ for D^+ ranges from ~ 2 keV to ~ 6 keV during ELMs which gives an average of ~ 4 keV. In these conditions, Fig. 1 shows that $Y_{D/W}$ ~ 0.02. It appears that W sputtering due to Be^{2+} and other Be species – all contributing in the same way - saturates in this domain of $E_{i,max}$ values and it will pessimistically be assumed that $Y_{Be/W}$ ~ 0.2 during ELMs. Since E_i ~ 0.1 keV in inter-ELM, $Y_{D/W}$ is negligible and $Y_{Be/W}$ ~ 0.01 (see Fig. 1) which confirms that W sputtered by Be^{2+} is the dominant sputtering process during this phase as already discussed in [4].

According to Fig. 3, the average OT perpendicular ion flux increases by a factor ~ 4 between the inter-ELM phase and the ELM phase and the Be concentration in the impinging target ion flux is ~ 1% [4]. Thus, if ion fluxes are normalized to the inter-ELM

D^+ flux, the typical variation of D^+ and Be^{2+} perpendicular OT target fluxes over a full ELM cycle the values calculated in Table 2 are obtained. The contribution to W sputtering due to both species can therefore be evaluated and compared. It appears that the W sputtering, normalized to the inter-ELM W sputtering level, is dominantly due to D^+ during ELMs (see Table 2). Estimates are only provided for the W sputtering source; the small fraction reaching the plasma core because of prompt W redeposition has not been estimated here.

If it is assumed that the inter-ELM phase is ~ 10 times longer than the ELM phase (Fig. 3), the integrated amount of W sputtered by Be^{2+} over an ELM cycle is an order of magnitude lower than the integrated amount of W sputtered by D^+, according to the estimates in Table 2. Thus, the choice of Be as plasma facing material for the main chamber seems to have very limited impact on W sputtering in the divertor in JET-ILW which is encouraging for ITER. However, W sources during ELMs are expected to increase with the mass of the main plasma species (e.g. DT and He plasmas), see Fig.1. The use of N, Ne or Ar impurity seeding for partially detached divertor operation to reduce the target heat flux is also expected to participate to W sputtering [16] but this case has not been studied here.

Mention has to be made that the sputtering yield used here (Fig. 1) have been calculated for normal incidence on the OT while in reality, the angle of incidence of D^+ and Be^{2+} on the OT are smaller than 90°, see [17]. However, this does not affect the normalized fluxes shown on Table 2 and discussed here.

6. Conclusions

Mitigated Type I ELMs, with 0.7 MJ of energy, expected in ITER for the baseline scenario with 500 MW of fusion power and Q = 10, are expected to be the dominant source of W in ITER. Very small amounts of W will be tolerated in the plasma core to ensure good performance [2]. Therefore, it is critical to predict accurately the W source due to ELM sputtering and this means that the energy of the incident ions needs to be known.

Coupled IR and LP measurements in JET-ILW H-mode experiments with ITER relevant ELM energy drop have been used here to confirm that D^+ have sufficient impact energy during ELMs to be the main responsible for W sputtering when no extrinsic impurity seeding is involved. In the series of discharges studied here, it appears that $E_{i,max}$ during ELMs is in the range 2 – 6 keV for D^+ and has a simple linear dependence on $T_{e,\max}^{ped}$. The use of N, Ne or Ar impurity seeding for target heat flux reduction is also expected to participate to W sputtering [16] but these cases were not investigated in the present work.

Comparison of LP with D_α ion flux measurements and analysis of reconstructed I-V characteristics during ELMs have been presented to prove that the ion current does

saturate in these conditions. Thus, J_{sat} measurements during ELMs are accurate and it was therefore reasonable to couple it to IR measurements for E_i estimates.

The saturation of the ion current measured by the LP during ELMs is possible thanks to the surprisingly low T_e of the order of 20 - 30 eV (inter-ELM conditions) found by the fit of the reconstructed I-V characteristic. These results are consistent with the predictions of the "Free-Streaming" model for the description of parallel ELM transport [12-14]. According to the model, electrons have to transfer most of their parallel energy to the ions on their way to the target to maintain the quasi-neutrality of the ELM filaments. The remaining low energy ELMy electrons are therefore easy to repel by the biased LP at the targets, making the ion flux measurement possible during ELMs.

This study indicates that the choice of Be as plasma facing material for the main chamber have very limited impact on W sputtering in the divertor in JET-ILW. Since the main species seems to be responsible for most of the W sputtering in H-mode unseeded JET-ILW experiments, W sources during ELMs are expected to increase with the mass of the main plasma species (e.g. DT and He plasmas) according to the standard formula for the physical sputtering yield.

Acknowledgments

This work has been carried out within the framework of the EUROfusion Consortium and has received funding from the European Union's Horizon 2020 research and innovation programme under grant agreement number 633053 and MSMT INGO grant LG14002. The views and opinions expressed herein do not necessarily reflect those of the European Commission.

References

[1] A. Loarte et al., Nucl. Fusion **54** (2014) 033007
[2] R. Dux et al., J. Nucl. Mater. **390-391** (2009) 858
[3] G.F. Matthews et al., 2011 Phys. Scr. 2011 014001
[4] S. Brezinsek et al., PSI 2014
[5] W. Eckstein et al., Report IPP 9/132 (2002)
[6] J.W. Coenen et al., PSI 2014
[7] D. Tskhakaya et al., J. Nucl. Mater. **415** (2011) S860–S864
[8] H.P. Summers. *Atomic data and analysis structure user manual*. University of Strathclyde, 2nd edition, 2004
[9] M.F. Stamp et al., Physica Scripta vol. **T91** (2001) 13
[10] R.A. Pitts et al., Nucl. Fusion **43** (2003) 1145–1166
[11] M. Wischmeier et al., J. Nucl. Mater. **363–365** (2007) 448–452
[12] W. Fundamenski et al., Plasma Phys. Control. Fusion **48** (2006) 109–156
[13] T. Eich et al., J. Nucl. Mater. **390–391** (2009) 760–763
[14] D. Moulton et al., Plasma Phys. Control. Fusion **55** (2013) 085003

[15] T. Eich et al., J. Nucl. Mater. **415** (2011) S856–S859
[16] G.J. van Rooij et al., J. Nucl. Mater. **438**, Supplement, (2013) S42–S47
[17] A. Kirschner et al., PSI 2014

Table Captions:

Table 1 List of unseeded H-mode JET-ILW discharges studied here

Table 2 Estimates of E_i, W sputtering yields, normalized ions and W fluxes in ELM and inter-ELM conditions

Figure captions:

Fig. 1 Curves of W sputtering yields due to Be in red, helium (He) in green, tritium (T) in magenta and deuterium (D) in blue

Fig. 2 Left: positions of LP and IR camera line of sight in JET-ILW divertor with the different Tile numbers. Right: magnetic equilibrium for #84782 at 13 s and position of D_α spectroscopy and ECE lines of sight in JET-ILW main chamber

Fig. 3 (a) Coherent averaging of total OT ion flux from LP (blue data points) and calibrated D_α spectroscopy (red data points) over the cumulated ELM cycles of #84782, (b) discrepancy between both curves

Fig. 4 (a) Coherent averaging of total OT heat flux measured by the IR camera over the cumulated ELM cycles of #84782, (b) same as previously with the intensity of D_α, Be II and W I line radiation (note that for convenience, the scale for Be II and W I is 100 time lower than the scale for D_α)

Fig. 5 I-V characteristic reconstruction obtained by cumulating I and V measurements taken by the LP in the peak ELMy ion flux of each ELM event over the discharge #84782

Fig. 6 Coherent averaging of T_e^{ped} measured by ECE over the cumulated ELM cycles of #84782

Fig. 7 Coherent averaging of (a) T_e^{ped} $q_\perp$ measured from IR for Probe 13 position, (b) J_{sat} measurement by Probe 13, (c) Ei deduced from LP and IR measurements, (d) intensity of W I line radiation over the cumulated ELM cycles of #84782

Fig. 8 $E_{i,max}/5$ in function of $T_{e,\max}^{ped}$ from coherent averaging of LP, IR and ECE measurements obtained in the discharges listed in Table 1

JET Pulse number	Average NBI power (MW)	Plasma current (MA)
#84589	12	2
#84593	12	2
#84613	13	2
#84614	13	2
#84722	20	3
#84724	19	3
#84778	21	3
#84779	21	3
#84782	21	3

Table 1

Phase	ELM Phase		Inter-ELM Phase	
Species	D^+	Be^{2+}	D^+	Be^{2+}
E_i (keV)	4	4	~ 0.1	~ 0.1
W sputtering yield	2.10^{-2}	2.10^{-1}	~ 0	10^{-2}
Normalized Γ_D (s^{-1})	4	4.10^{-2}	1	10^{-2}
Normalized Γ_W (s^{-1})	8.10^{2}	8.10^{1}	~ 0	1

Table 2

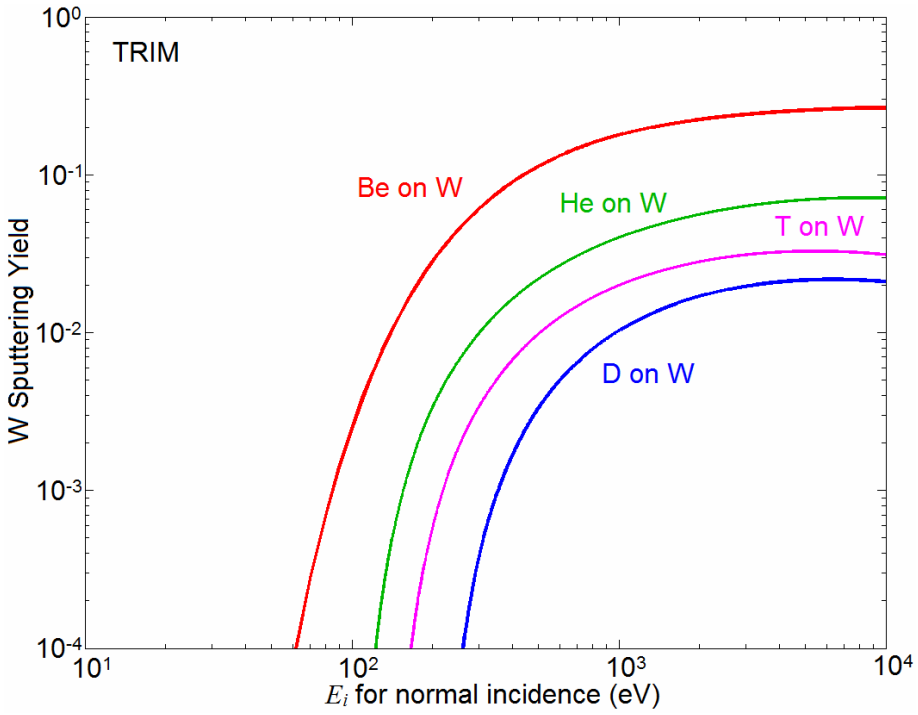
TRIM
Be on W
He on W
T on W
D on W
W Sputtering Yield
E_i for normal incidence (eV)
10^0
10^{-1}
10^{-2}
10^{-3}
10^{-4}
10^1
10^2
10^3
10^4

Figure 1

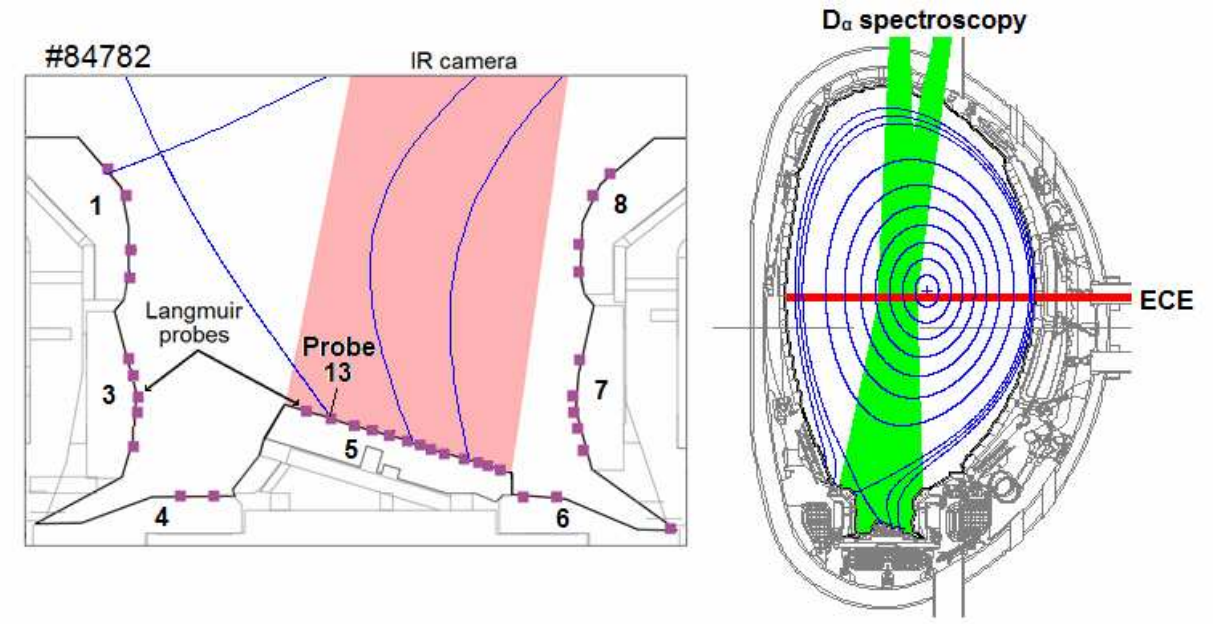
#84782
IR camera
1
Langmuir
probes
3
Probe
13
5
4
6
8
7
Dα spectroscopy
ECE

Figure 2

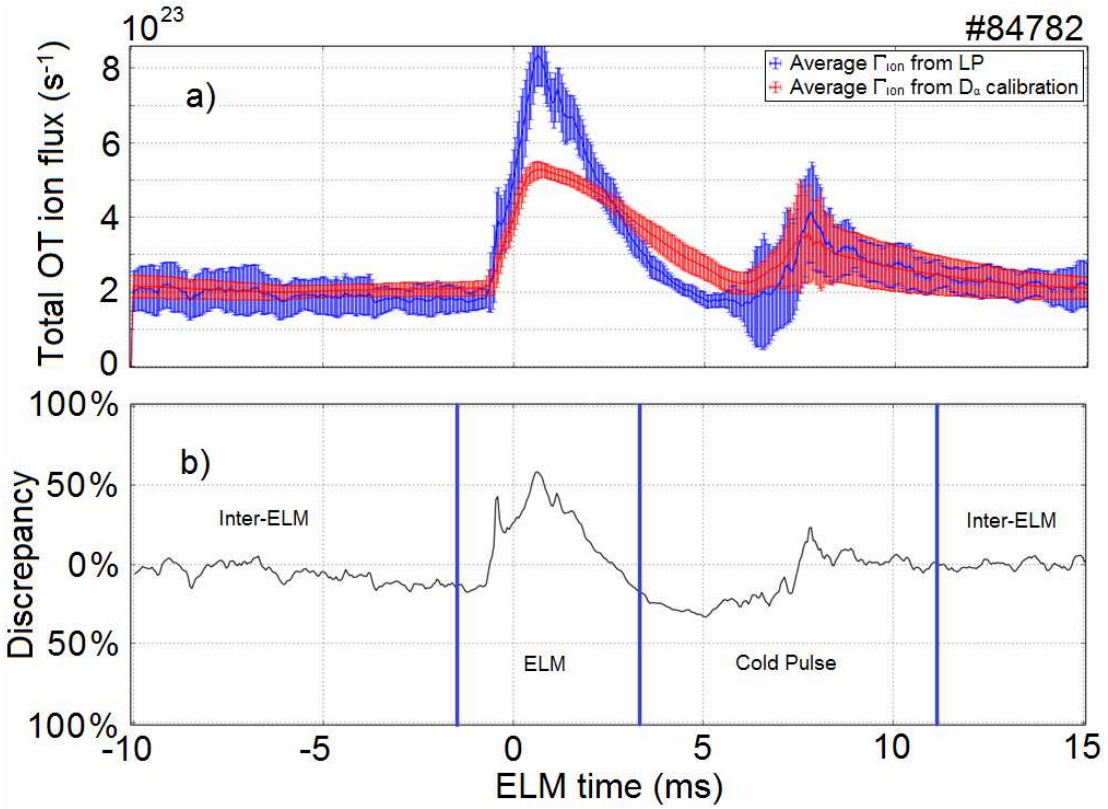
#84782
a)
Average Γion from LP
Average Γion from Dα calibration
Total OT ion flux (s-1)
10^23
8
6
4
2
0
b)
Inter-ELM
ELM
Cold Pulse
Inter-ELM
Discrepancy
100%
50%
0%
50%
100%
-10
-5
0
5
10
15
ELM time (ms)

Figure 3

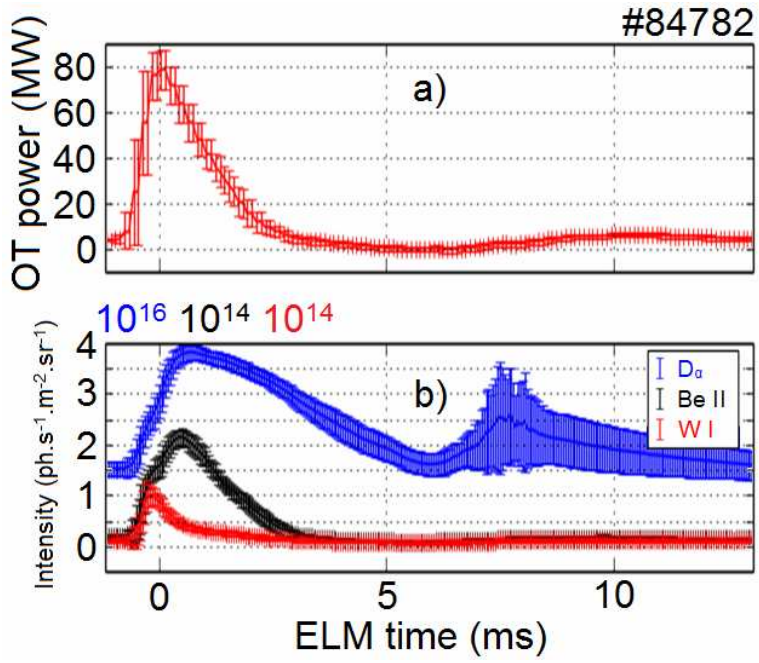
#84782
OT power (MW)
80
60
40
20
0
a)
10^16 10^14 10^14
Intensity (ph.s^-1.m^-2.sr^-1)
4
3
2
1
0
b)
Dα
Be II
W I
0
5
10
ELM time (ms)

Figure 4

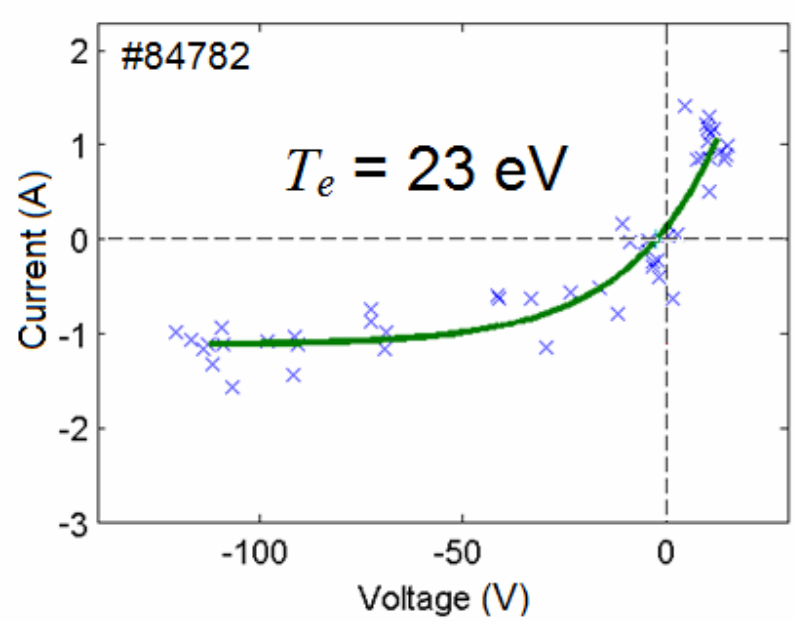

Figure 5

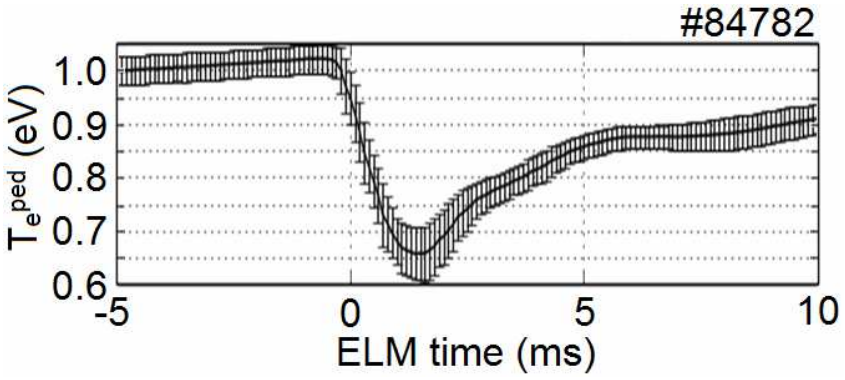

Figure 6

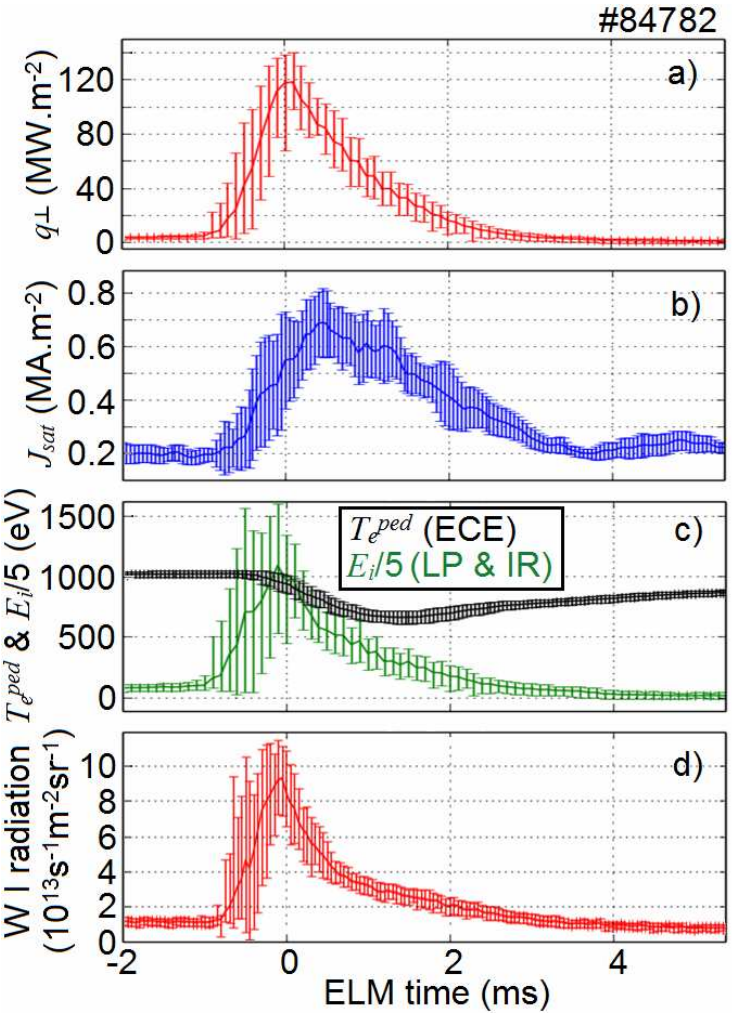
#84782
a)
$q_\perp$ (MW.m^{-2})
120
80
40
0
b)
J_{sat} (MA.m^{-2})
0.8
0.6
0.4
0.2
c)
T_e^{ped} (ECE)
E_i/5 (LP & IR)
T_e^{ped} & E_i/5 (eV)
1500
1000
500
0
d)
W I radiation
(10^{13}s^{-1}m^{-2}sr^{-1})
10
8
6
4
2
0
-2
0
2
4
ELM time (ms)

Figure 7

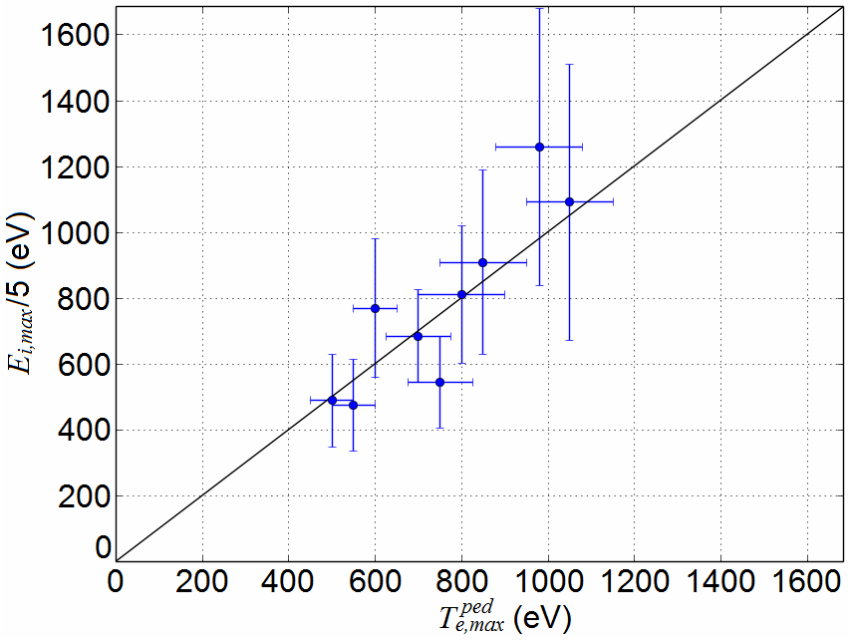
1600
1400
1200
1000
800
600
400
200
0
$E_{i,max}/5$ (eV)
0
200
400
600
800
1000
1200
1400
1600
$T_{e,max}^{ped}$ (eV)

Figure 8